# Explosive Bifurcation to Chaos in Weakly Coupled Semiconductor Superlattices

K. J. Luo, H. T. Grahn, and K. H. Ploog
*Paul-Drude-Institut für Festkörperelektronik, Hausvogteiplatz 5-7, D-10117 Berlin, Germany*

L. L. Bonilla
*Escuela Politécnica Superior, Universidad Carlos III de Madrid, Butarque 15, E-28911 Leganés, Spain*
(Received 12 February 1998)

The bifurcation scenario to chaos has been studied for vertical transport in an incommensurately driven superlattice system. With increasing driving amplitude, quasiperiodic, frequency-locked, and chaotic oscillations are identified by using Poincaré maps, which show a variety of attractors in the chaotic regime. The dimension of the attractor is abruptly increased in the transition process, i.e., the bifurcation between frequency locking and chaos is explosive. However, the bifurcation pattern depends strongly on the applied dc bias, providing clear evidence that the system is spatially inhomogeneous in the vertical direction. [S0031-9007(98)06837-9]

PACS numbers: 73.50.Fq, 73.20.Dx, 73.40.Gk

Spatiotemporal chaos has been studied both experimentally and theoretically in liquid and chemical systems [1], in coupled map lattices [2], as well as in solid-state systems [3–7]. When the investigated system is driven by an incommensurate frequency, i.e., the ratio of the natural frequency and the driving frequency is an irrational number, the transition to chaos has been predicted theoretically to occur via the following routes: either quasiperiodicity → frequency locking → chaos or directly from quasiperiodicity to chaos [2–5]. Both routes to chaos have been observed in a number of experiments [3–5].

Vertical transport in weakly coupled semiconductor superlattices (SL's) is known to exhibit nonlinear phenomena such as domain formation [8–10], multistability [11], and self-sustained current oscillations [12–14]. It has been shown that the self-sustained current oscillations are due to a quasi-one-dimensional motion of the domain boundary in the SL direction, i.e., vertical to the SL layers [8,12–15]. Therefore, the temporal behavior of the current oscillations is directly related to the vertical spatiotemporal motion of the domain boundary inside the SL. Theoretical studies predict the appearance of chaos in such SL systems accompanied by the breakdown of spatiotemporal coherence of the motion of the domain boundary [15]. Although driven and undriven chaos of these current oscillations have been recently observed in the frequency power spectra [16], little is known about the transition process between synchronization (frequency locking) and chaos as well as the actual type of chaotic behavior in the experimentally investigated SL system. This type of information can be obtained only from real-time measurements.

In this paper, we present Poincaré maps in the presence of an external driving voltage applied parallel to the growth direction of a weakly coupled semiconductor SL. These Poincaré maps clearly indicate that the transition from frequency locking to chaos is accompanied by a loss of spatiotemporal coherence. Furthermore, the Poincaré maps reveal that a number of attractors with varying complexity exist in the chaotic regime. However, for different dc biases, completely different routes to chaos are observed. At the same time, the observed bifurcation patterns are more complicated than the ones predicted by the theoretical investigation reported in Ref. [15]. The experimental discrepancy with the theory as well as the different observed routes to chaos may be due to the spatial inhomogeneity of the SL in the growth direction.

The investigated sample consists of a doped, 40-period, weakly coupled SL with 9.0 nm GaAs wells and 4.0 nm AlAs barriers. For a more detailed description of the structure and contact layers, see Refs. [16,17]. The dc and ac electric fields are applied in parallel to the SL direction. The experimental data are recorded in a He-flow cryostat at 5 K using high-frequency coaxial cables with a bandwidth of 20 GHz. The driving voltage in the form of $V_{\mathrm{ac}}\sin(2\pi f_d t)$ is generated with a Wavetek 50 MHz pulse/function generator (model 81), where $f_d$ denotes the driving frequency. The power spectra of the current oscillations are detected with an Advantest R3361 spectrum analyzer. The real-time current traces are recorded with a Hewlett-Packard 54720A digital oscilloscope, which is triggered by the synchronization signal from the pulse/function generator, using a sampling rate of 1 GSa/s and 32 768 points/snapshot. The resulting time resolution was about 20–50 points per period $\tau_d$ of the driving frequency, which corresponds to about 600–1600 $\tau_d$ per snapshot.

The dc bias $V_{\mathrm{dc}}$ is fixed at two different voltages in the second plateau of the time-averaged current-voltage characteristic, where current oscillations due to a recycling motion of a charge monopole have been observed [14]. Without any ac driving voltage, the system exhibits periodic self-sustained current oscillations with an intrinsic fundamental frequency $f_0 = f_i(V_{\mathrm{ac}} = 0)$ of 30.5 MHz at $V_{\mathrm{dc}} = 6.574$ V and 11.4 MHz at 7.080 V. In the following, we will fix $f_d$ at $f_0 \times (1 + \sqrt{5})/2$ (the golden mean) and vary $V_{\mathrm{ac}}$ to study the bifurcation scenario to chaos. Figure 1 shows the bifurcation diagrams of the

 0031-9007/98/81(6)/1290(4)$15.00 © 1998 The American Physical Society

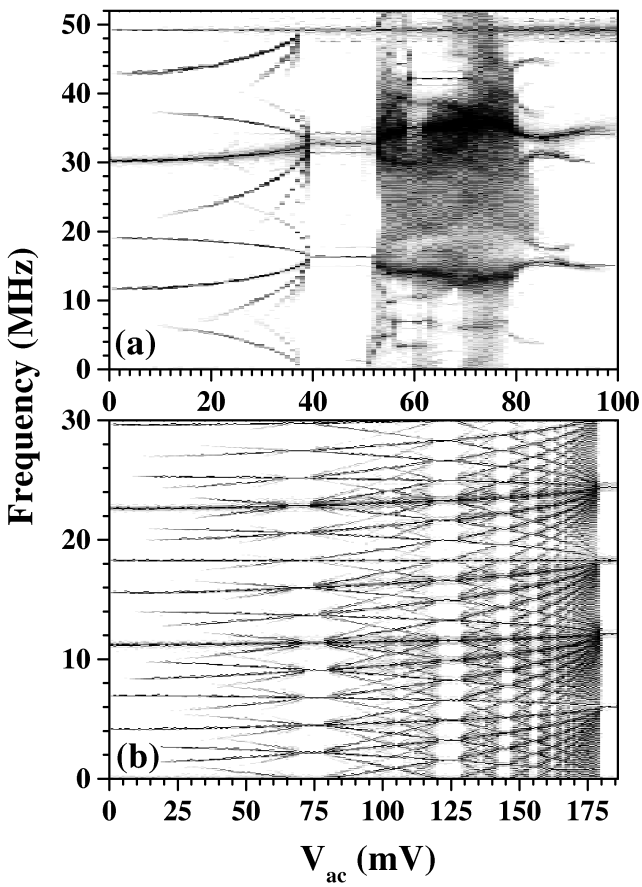


FIG. 1. Frequency bifurcation diagram for $V_{dc} = 6.574$ V and $f_d = 49.4$ MHz (a) as well as for $V_{dc} = 7.080$ V and $f_d = 18.4$ MHz (b) recorded at 5 K. The current power spectra are shown as density plots vs the amplitude of the driving voltage $V_{ac}$, where dark areas correspond to large amplitudes.

power spectra as a function of $V_{ac}$ for the above values of $V_{dc}$. The frequency of the driving voltage $f_d$ is set to 49.4 MHz in Fig. 1(a) and 18.4 MHz in Fig. 1(b). When the driving voltage is superimposed on the dc voltage, quasiperiodic oscillations are observed in both power spectra, since $f_0$ and $f_d$ are incommensurate. However, there are large differences in the two power spectra for larger values of $V_{ac}$. In Fig. 1(a), when $V_{ac}$ becomes larger than 38 mV, the power spectra smear out over a narrow frequency band around three peaks indicating a transition from quasiperiodicity to synchronized chaos, but the chaotic window is very narrow. When $V_{ac}$ is increased further, the system enters a frequency-locked state with a winding number of $2/3$. For $V_{ac}$ larger than 51 mV, the power spectra become continuous over a much larger range of $V_{ac}$. At the same time, the frequencies are distributed over a much wider range (up to more than 50 MHz), indicating that the system has entered a more complex chaotic state. The power spectrum in Fig. 1(b) has a much higher symmetry. Frequency-locked and quasiperiodic windows alternate with increasing $V_{ac}$. The winding number of the frequency-locked states increases according to $(2n + 1)/(3n + 2)$ with $n = 2, 3, 4, 5, \ldots$. It finally reaches $2/3$ for very large values of $V_{ac}$. In contrast to Fig. 1(a), the power spectra do not smear out before a frequency-locked window is reached, only the spacing between adjacent frequency peaks is reduced.

In order to obtain more insight into the transition from frequency locking to chaos, Poincaré maps (first return maps) have been derived from the real-time current oscillation traces. Figure 2 shows three examples of current traces recorded under the same conditions as in Fig. 1(a). At 34 mV, the oscillations are quasiperiodic, at 40 mV they are frequency locked, and at 63 mV they are chaotic. These assignments will be proven below using Poincaré maps, which give information about the structure of an attractor in a dissipative system [3,15]. Poincaré maps are constructed by plotting $I_{n+1}$ as a function of $I_n$, where $I_n$ is obtained by sampling the current trace $I(t)$ at a fixed phase (the maximum of the amplitude of the driving frequency signal) in the $n$th period of the driving voltage. Figure 3 shows Poincaré maps obtained at the dc bias of 6.574 V. When $V_{ac}$ is small (9 to 34 mV), the Poincaré maps are smooth loops indicating quasiperiodic oscillations [2–4,7,15]. However, when $V_{ac}$ reaches 38 mV, the loop splits up into three extended branches as shown for 39 mV in Fig. 3, which collapses into three points at 40 mV, demonstrating frequency locking. The extended branches at 38–39 mV are an indication of the appearance of *synchronized chaos*, i.e., the chaotic behavior is confined to three narrow frequency bands, which can also be seen in the power spectra in Fig. 1(a). Such a chaotic orbit

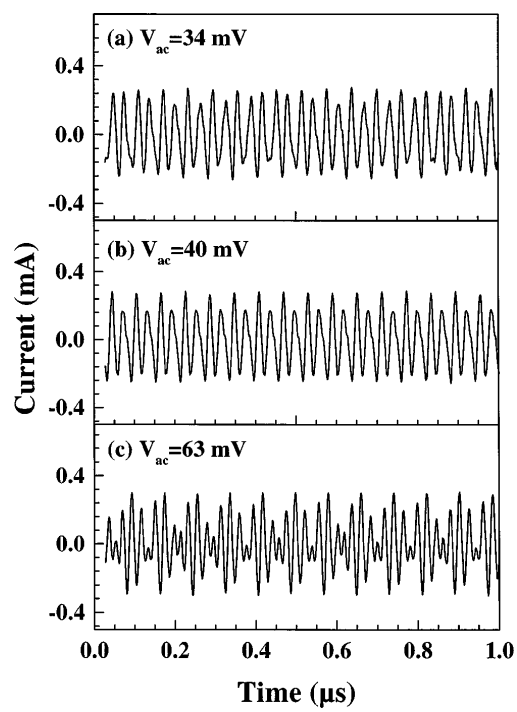


FIG. 2. The ac component of the current vs time for several driving amplitudes $V_{ac}$ as indicated for the same conditions as in Fig. 1(a). (a) 34 mV, (b) 40 mV, and (c) 63 mV.

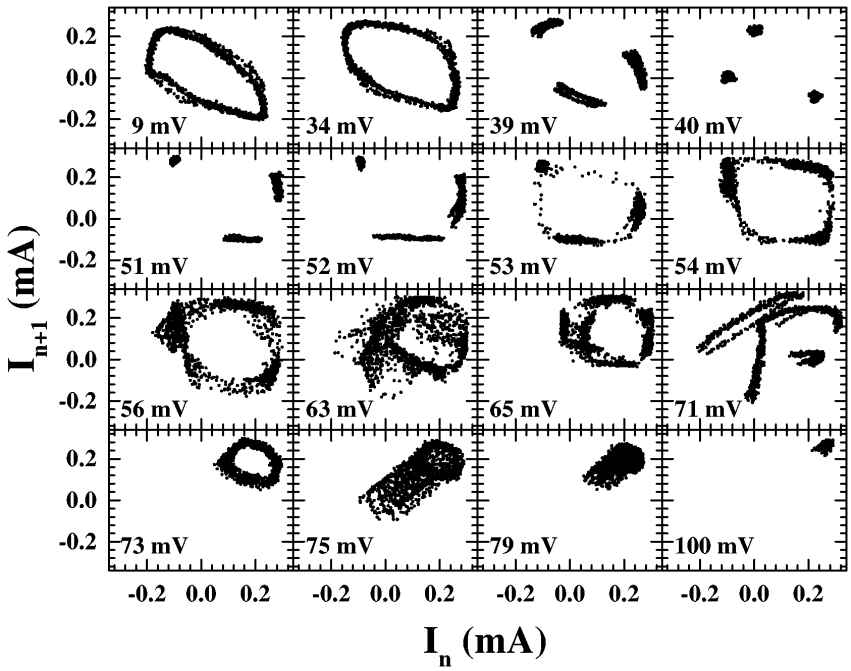


FIG. 3. Poincaré maps for different driving amplitudes $V_{ac}$, as indicated, obtained from current oscillation traces recorded for the same conditions as in Fig. 1(a).

may exist at the edge of the so-called *Arnol'd tongue* in the $V_{ac} - f_0/f_d$ phase diagram and is very close to a period-3 locking state [15]. Increasing $V_{ac}$ slightly, the system enters the frequency-locked state at 40 mV. This frequency-locked state exists until $V_{ac}$ reaches 51 mV, where two of the three points in the Poincaré map begin to extend into branches demonstrating the onset of chaos. Between 51 and 54 mV, these branches eventually become connected with each other (cf. Fig. 3). Since the current oscillations are caused by the spatiotemporal motion of the domain boundary in the SL [13–16], the expansion of the three points into branches clearly demonstrates that the vertical motion of domain boundary loses its spatiotemporal coherence during the bifurcation process from frequency locking to chaos.

The Poincaré maps between 51 and 54 mV in Fig. 3 show that the bifurcation from frequency locking to chaos is explosive, i.e., it is accompanied by an abrupt increase of the attractor dimension. In this type of bifurcation process, the dimension of the attractor is expanded from isolated points (zero-dimensional object) into an object with a finite dimension. Moreover, within the chaotic regime, the complexity of the chaotic attractor increases with a small change of $V_{ac}$. When $V_{ac}$ is beyond 54 mV, the structure of the Poincaré maps in Fig. 3 becomes more complex. As shown in Fig. 3, a number of different chaotic attractors are revealed for $V_{ac}$ between 56 and 79 mV. A further increase of $V_{ac}$ results in a transition from a chaotic to a 1:1 frequency-locked state, as shown in Fig. 3 for $V_{ac} = 100$ mV.

The bifurcation route to chaos described above can be summarized as follows: quasiperiodicity → synchronized chaos → frequency locking → chaos → chaos with higher complexity. However, when $V_{dc}$ is fixed to 7.080 V, we observe a very different route to chaos. The corresponding bifurcation diagram of the power spectra has already been described above. The Poincaré maps for the regions in the power spectra corresponding to frequency-locked states and quasiperiodic oscillations agree with the interpretation obtained from the power spectra. Figure 4 shows several Poincaré maps for driving amplitudes between 155 and 180 mV, where the power spectra become quasicontinuous. At 155 mV, the Poincaré map shows 17 points indicating frequency locking, in agreement with

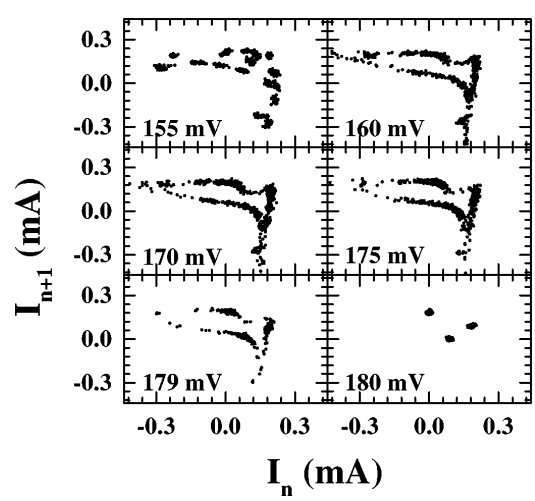


FIG. 4. Poincaré maps for several driving amplitudes $V_{ac}$ between 155 and 180 mV obtained from current oscillation traces for the same conditions as in Fig. 1(b).

the winding number 11/17 obtained from the power spectra. At 160 mV, the Poincaré map becomes a twisted loop with a varying point density, which may originate from a chaotic attractor. This structure remains almost unchanged until $V_{ac}$ reaches 175 mV. Between 175 and 180 mV, the system undergoes a transition to frequency locking with a winding number of 2/3, as shown by the Poincaré map for 180 mV, which contains only three points. This bifurcation process can also be considered explosive due to the abrupt change of the attractor dimension. The bifurcation to chaos observed for this applied dc voltage corresponds to the typical route consisting of quasiperiodicity → frequency locking → quasiperiodicity → ... → frequency locking → chaos. However, in contrast to the bifurcation scenario observed at $V_{dc} = 6.574$ V, there is no evidence for a window containing synchronized chaos at $V_{dc} = 7.080$ V. This result agrees with the observed difference in the power spectra of Fig. 1.

The route to chaos at 7.08 V is completely different from the one observed at 6.574 V, but similar to the one in our previous report [16], where a different mesa from the same wafer was studied. Note that, in all previous works, real-time traces with sufficient resolution to derive Poincaré maps were not available so that the type of chaos derived from frequency spectra alone could not be determined unambiguously. Furthermore, the theoretical study of Ref. [15] did not reveal such a complicated bifurcation pattern either. Only the Poincaré maps can reveal the structure of the chaotic attractors, which is much richer for the experimentally investigated system. The discrepancy between experiment and calculation may originate from the structural imperfection of the SL. The calculation in Ref. [15] is based on a perfect SL with identical well and barrier widths and doping density, as well as electron drift velocity for all periods, i.e., for an ideal SL, which is spatially homogeneous in the growth direction. However, in a real SL system, the fluctuations of well and barrier width, as well as the doping density, can disturb the perfection of the SL, as reported for static domains in Ref. [18,19]. It has already been shown theoretically that imperfections will strongly affect the oscillatory behavior of such a system [20]. Therefore, for an inhomogeneous SL, the oscillatory behavior will also strongly depend on the exact location of the oscillating domain boundary inside the SL. Since for different dc biases the oscillating domain boundary will cover different regions of the SL (cf. Ref. [14]), the different oscillatory behavior at 6.574 and 7.08 V may indicate that the SL is imperfect in the growth direction. The imperfection of the SL would substantially increase the number of degrees of freedom that are necessary to model the experimental system. Another possibility for the different observed routes to chaos is the influence of the contact layers. For 6.574 V, the domain boundary oscillates near one of the contacts, while for 7.08 V, the domain boundary is oscillating closer to the center of the SL (cf. Ref. [14]). So far, the contact layers have only been included in the simulations in a very simple way so that the observed effects are not included in the simulations.

In summary, we have studied different bifurcation scenarios to chaos in an incommensurately driven SL by evaluating Poincaré maps from real-time current traces and comparing them with measured power spectra. The difference in the bifurcation patterns for different dc bias voltages gives direct evidence for the existence of imperfections in the growth direction of the SL. A nonlinear system is particularly sensitive to imperfections. It supports our previous assumption that the experimentally investigated SL represents a system with a much larger number of degrees of freedom than the corresponding perfect SL.

The authors would like to thank A. Fischer for sample growth, H. Kostial for technical assistance, and O. M. Bulashenko, F.-J. Niedernostheide, and S. Teitsworth for valuable discussions. The partial support of the Deutsche Forschungsgemeinschaft within the framework of Sfb 296 is gratefully acknowledged.

[1] M. C. Cross and P. C. Hohenberg, Rev. Mod. Phys. **65**, 851 (1993).
[2] J. Crutchfield and K. Kaneko, in *Directions in Chaos*, edited by Hao Bai-lin (World Scientific, Singapore, 1987), Vol. 1, p. 272.
[3] G. A. Held and C. Jeffries, Phys. Rev. Lett. **55**, 887 (1985); *ibid.* **56**, 1183 (1986).
[4] E. G. Gwinn and R. M. Westervelt, Phys. Rev. Lett. **57**, 1060 (1986); *ibid.* **59**, 157 (1987).
[5] A. M. Kahn, D. J. Mar, and R. M. Westervelt, Phys. Rev. Lett. **68**, 369 (1992).
[6] K. Aoki and K. Yamamoto, Appl. Phys. A **48**, 111 (1989).
[7] F.-J. Niedernostheide, M. Ardes, M. Or-Guil, and H.-G. Purwins, Phys. Rev. B **49**, 7370 (1994); F.-J. Niedernostheide *et al.*, *ibid.* **54**, 14 012 (1996).
[8] L. L. Bonilla, in *Nonlinear Dynamics and Pattern Formation in Semiconductors and Devices*, edited by F.-J. Niedernostheide (Springer-Verlag, Berlin, 1995), Chap. 1.
[9] K. K. Choi *et al.*, Phys. Rev. B **35**, 4172 (1987).
[10] H. T. Grahn, R. J. Haug, W. Müller, and K. Ploog, Phys. Rev. Lett. **67**, 1618 (1991).
[11] J. Kastrup *et al.*, Appl. Phys. Lett. **65**, 1808 (1994).
[12] S. H. Kwok *et al.*, Phys. Rev. B **51**, 10 171 (1995).
[13] J. Kastrup *et al.*, Phys. Rev. B **52**, 13 761 (1995).
[14] J. Kastrup *et al.*, Phys. Rev. B **55**, 2476 (1997).
[15] O. M. Bulashenko and L. L. Bonilla, Phys. Rev. B **52**, 7849 (1995); O. M. Bulashenko, M. J. García, and L. L. Bonilla, *ibid.* **53**, 10 008 (1996).
[16] Y. Zhang *et al.*, Phys. Rev. Lett. **77**, 3001 (1996); Y. Zhang, R. Klann, H. T. Grahn, and K. H. Ploog, Superlattices Microstruct. **21**, 565 (1997).
[17] H. T. Grahn, in *III-V Quantum System Research*, edited by K. Ploog, IEE Materials and Devices Series 11 (IEE, Stevenage, 1995), p. 329.
[18] A. Wacker *et al.*, Phys. Rev. B **52**, 13 788 (1995).
[19] G. Schwarz *et al.*, Appl. Phys. Lett. **69**, 626 (1996).
[20] E. Schöll *et al.*, in *Hot Carriers in Semiconductors*, edited by K. Hess *et al.* (Plenum Press, New York, 1996), p. 177.